Simple Numerical Model (PRAM) for Simulation of the Passenger–Bag Interactions During Deployment of an Airbag

RAMESH KESHAVARAJ,[1] RICHARD W. TOCK,[1] GUY S. NUSHOLTZ[2]

[1] Polymer Processing and Testing Laboratory, Department of Chemical Engineering, Texas Tech University, Lubbock, Texas 79409-43121

[2] Chrysler Technology Center, Chrysler Corporation, Auburn Hills, Michigan 48326-2757

Received 10 October 1995; accepted 27 July 1997

ABSTRACT: The pressure-time history of a deployed airbag provides the basis for the restraint created by this safety system. A simple numerical simulation of this pressure–time history was developed based on our understanding of the various factors that influence the restraint performance. The general interaction forces between the passenger and the airbag can be analyzed using this model. This article discusses some of the complex issues pertaining to the interaction forces between the occupant and the airbag. The predictions provided by the proposed numerical passenger restraint action model are in good agreement with published, experimental data. © 1998 John Wiley & Sons, Inc. J Appl Polym Sci **67:** 933–948, 1998

Key words: airbags; nylon; polyester; simulation; passenger restraint action model (PRAM); pressure–time history; forces of interaction; fabric-material response model (FMRM); kinetic energy adsorption model (KEAM)

INTRODUCTION

One of the newer passive restraint systems that mitigates the forces of impact in automobile collisions is commonly referred to as an airbag. Because of commercial television and the airbag's success rate, almost everyone is familiar with airbags. Conceptually, the performance of airbags is simple: a bag made of a soft fabric is inflated to a pillow and then dissipates the energy released during an accident. Behind this simple concept, however, the engineering embodied is very specific and complex. Many attempts have been made to simulate the airbag pressure–time history in the past. Most of these were based on thermodynamic theories.[1–8] Even though some of the models can simulate a time history that agrees with experimental evaluations, the factors affecting the energy dissipation in an airbag during its interaction with the occupant has not been adequately addressed. This area in safety restraints is addressed in this article with a simple numerical model.

The airbag pressure–time profile was simulated to facilitate this analysis. Many of the important factors affecting airbag response have been addressed in our earlier publications.[9–15] For example, an accurate fabric-material response model (FMRM) was developed based on artificial neural networks.[16] This model for the fabric behavior was then integrated with a kinetic energy adsorption model (KEAM) to analyze the relationships between the viscous and viscoelastic effects on energy dissipation with respect to the fabric properties.[15] The outputs from these two models were utilized to develop a numerical simulation that helps analyze passenger–airbag inter-

Correspondence to: R. Keshavaraj, R & D, Global Airbags, Milliken & Co., LaGrange, GA 30240.

Journal of Applied Polymer Science, Vol. 67, 933–948 (1998)
 CCC 0021-8995/98/050933-16

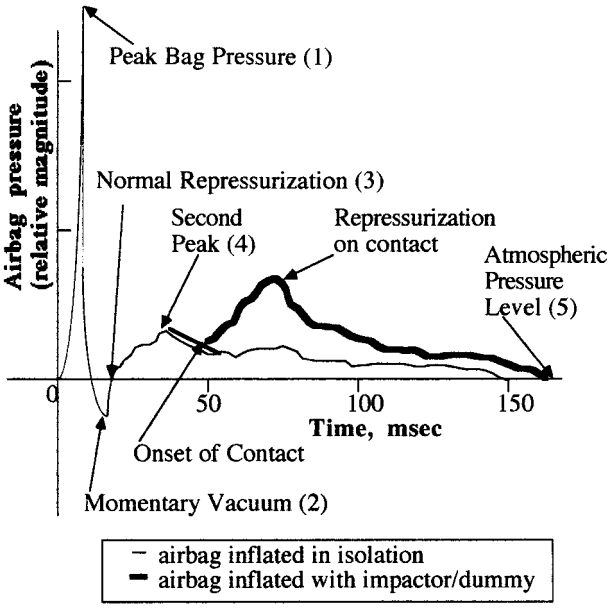

Figure 1 Airbag pressure waveform of an airbag deployed in isolation and with an impactor/dummy.

actions on a driver-side airbag. Simulations presented in this article relate to the driver-side airbag; however, a similar analysis can be carried out for a passenger-side airbag.

AIRBAG PRESSURE–TIME HISTORY

Comparisons of typical airbag pressure waveforms are shown graphically for an airbag inflation in isolation and for inflation followed immediately with an impactor/dummy (Fig. 1). Five different phases observed in this time history are marked in this figure. When the airbag is inflated in isolation, an initial peak bag pressure (1) is reached. After this initial peak is reached, a momentary vacuum (2) occurs in the bag, followed by subsequent normal repressurization (3). A second peak (4) is attained within approximately 30 msec, after which the bag pressure gradually decreases until atmospheric pressure is reached (5). In comparison, the pressure–time history with an impactor/dummy depicts the bag being pressurized by contact. Physical contact with the slowly deflating airbag accelerates gaseous outflow from the bag and thereby helps it to dissipate the kinetic energy of the passenger. The gaseous outflow generally is through the fabric or from specially constructed vents. A small fraction of energy can also be absorbed by mechanical stretching of the fabric's fibers. However, the fabric's permeability and/or vent system is of primary importance to energy dissipation.[15] In practice, the bag-pressure increase is typically in the range of 34–48 kPa. The permeability and biaxial performance of the various commercial fabrics were investigated in this range and reported in our earlier publications.[9,12,13]

FACTORS AFFECTING AIRBAG PRESSURE–TIME HISTORY

The interaction between the airbag and the occupant is a very complex process, and any attempt to accurately model the physical interactions between the passenger and the airbag requires many assumptions. The factors that affect the airbag pressure–time history can be broadly classified into five categories pertaining to: the airbag, the gas exhaust, the gas inflow characteristics, the airbag reaction surface, and dummy/impactor properties. The major factor that defines bag characteristics is the volume of the bag required for a particular fabric of choice. This can be evaluated by the KEAM model.[15] The shape of the bag, however, has only a minor influence on the pressure-time history[6] because, ultimately, the amount of the inflating gas and its temperature govern the energy dissipation. The gas exhaust characteristics are affected by the permeability of the fabric, seams, and vents and the total surface area. The permeability of a given fabric, the seam of an airbag, and the gas flow through the vent can be estimated by the technique championed by Chrysler and developed in our laboratories called blister inflation.[17] For example, the permeability–temperature–pressure drop relationship for a 630 denier (D) nylon 6,6 fabric with a 35 $\times$ 35 weave count is shown in Figure 2. Permeability data are displayed in this figure over a temperature and pressure drop range of 281–373 K and 3.4–200 kPa, respectively. It should be remembered that the biaxial deformation of the airbag fabrics cannot be determined *a priori* with the knowledge of the physical characteristics of the fabrics alone. Numerous fiber characteristics play a synergistic role in the observed deformation under biaxial conditions. Permeability behavior of a seam and vent from a driver-side airbag is also shown in Figures 3 and 4 for comparison purpose.[15] While the vents are normally circular in shape, a linear relationship

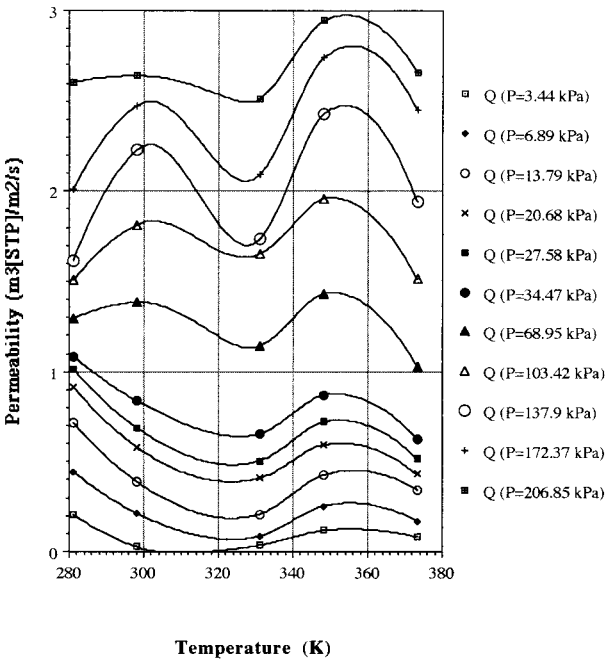

Figure 2 Permeability–temperature–pressure drop relationship for a 420 denier nylon 6,6 fabric.

between the differential pressure and the volumetric flow rate of the exhaust gas was observed between vents of 0.5–1.0 in. in diameter.[17] The gas dynamics are most affected by the flow rate of the gas and its temperature. The effect of both of these factors can be analyzed with the proposed simulation.

DEVELOPMENT OF PASSENGER RESTRAINT ACTION MODEL

In order to study the passenger restraint action during deployment of an airbag the pressure-time history of the inflation process was first simulated. A schematic of various components in the proposed numerical model is shown in Figure 5. The model proposed here consists of a circular cylinder with a diameter equal to the airbag's diameter, D_A (m), a flat impactor, and an airbag of volume, V_B (m^3). The impactor mass, m_I (kg), and area, A_I (m^2), correspond to the passenger/occupant during the simulated crash. It is assumed that the impactor forms a tight seal with the walls of the cylinder so that the exhaust gas from the airbag (through fabric, vents, and seams) is released to the atmosphere only though the vent of area, A_V (m^2). This vent is located at the bottom of the cylinder. During operation, when the impactor traveling at a velocity, v_I (m/s), comes in contact with the inflating airbag, the displacement of the impactor X (m) compresses the gases in the bag. Hence, the bag pressure, P_B (N/m^2), increases, forcing the gases to exhaust.

From the schematic, the change in the volume of the airbag, V_B, can be related to the displacement of the impactor, X, by the following relationship:

$$\frac{dV_B}{dt} = -(A_{eff} \cdot v_I) \qquad (1)$$

where A_{eff} is the effective area of contact (m^2) between the impactor and the airbag and v_I (m/s) is the velocity of the impactor. The negative sign

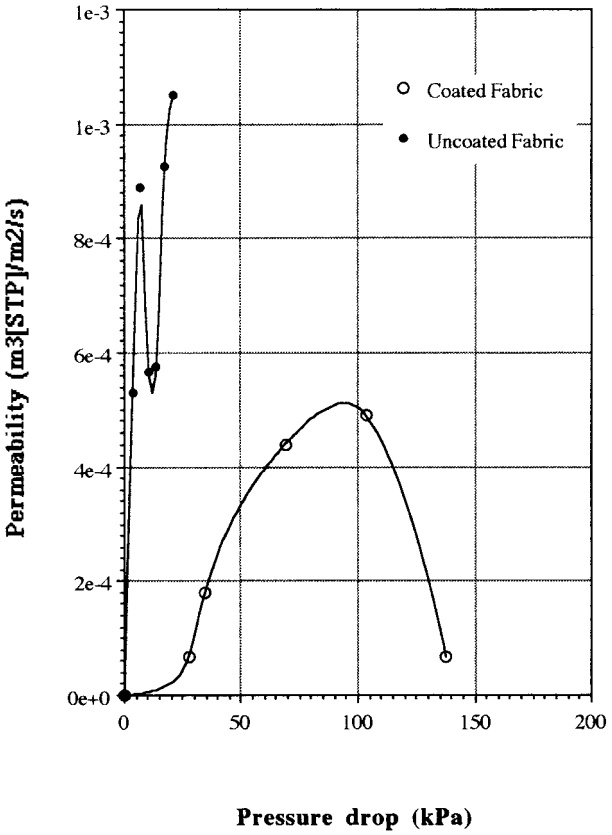

Figure 3 Permeability through seam in a driver-side airbag at ambient temperature.

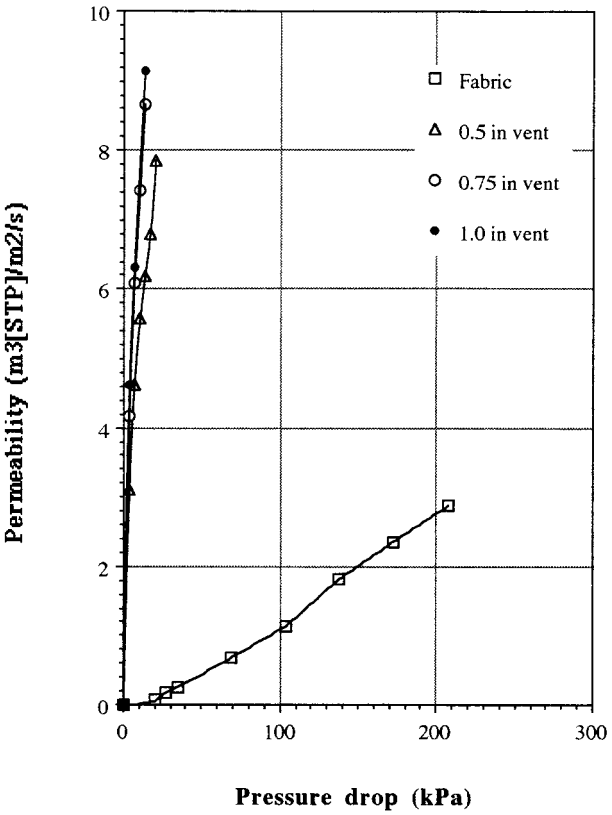

Figure 4 Effect of the airbag vent area on exhaust characteristics.

indicates a reduction in bag volume. The effective area of contact between the airbag and the impactor can be written again in terms of the displacement of the impactor, X (m). The original relationship used by Nefske[1] was used in this model:

$$\frac{\Delta A_{eff}}{\Delta X} = 41.666 \tag{2}$$

where the displacement ΔX is in inches and ΔA_{eff} is in square inches. This relationship was corrected to SI units in the model.

Thus, forces exerted by the airbag on the impactor can be estimated from the knowledge of the airbag pressure and the effective area of contact between them.

$$F_A = (P_B - P_A) \cdot A_{eff} \tag{3}$$

Here, F_A is the force (N) exerted by the airbag on the impactor, P_B (N/m^2) is the airbag pressure,

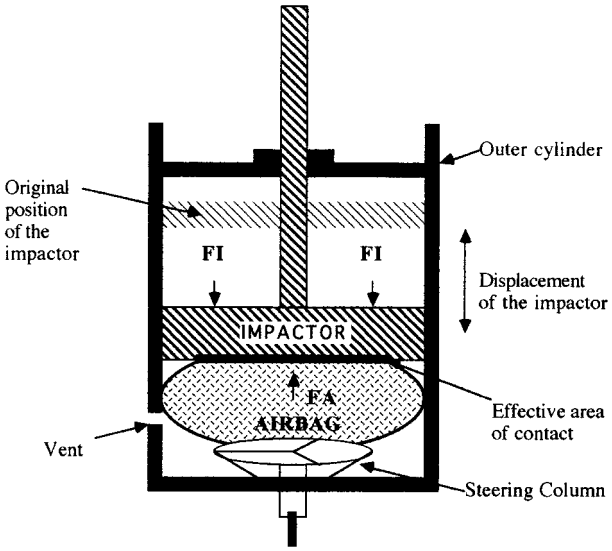

Figure 5 Schematic of the proposed model (PRAM).

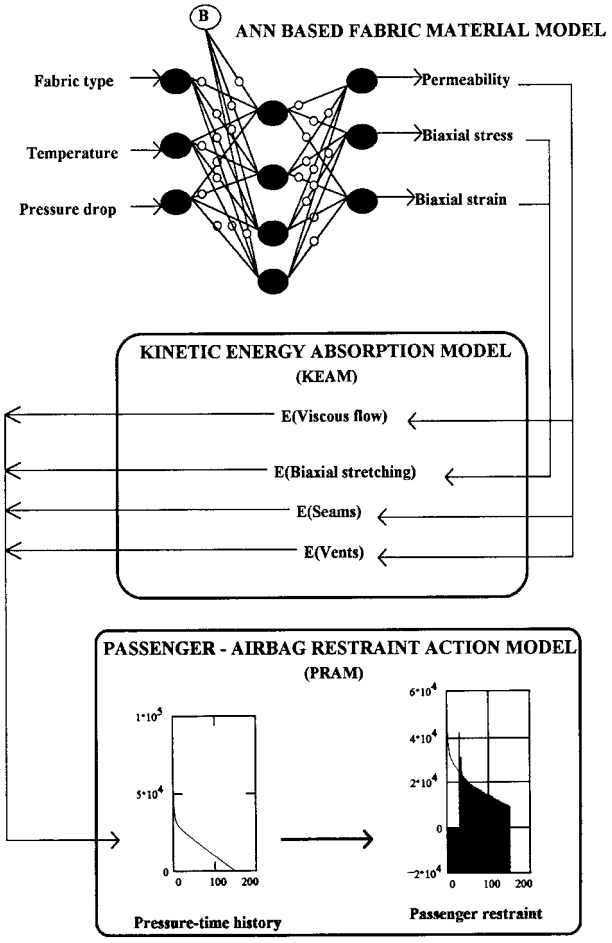

Figure 6 System integration of various airbag models.

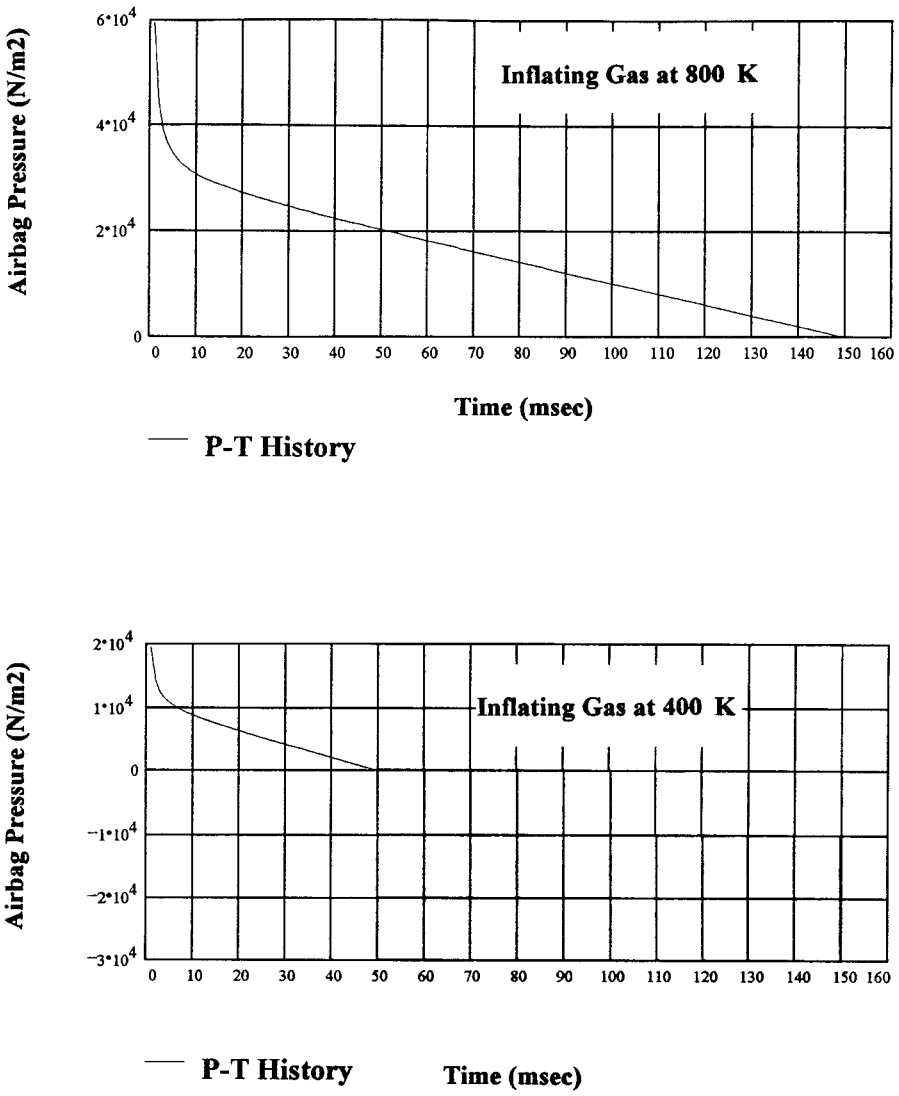

Figure 7 Simulation of the airbag pressure–time history.

P_A (N/m^2) is the atmospheric pressure, and A_{eff} (m^2) is the effective area of contact between the airbag and the impactor. It is important to note that this area changes with displacement, as given by the relation in eq. (2).

In a similar fashion, the force exerted by the impactor on the airbag can be estimated from the knowledge of the mass, velocity, and displacement of the impactor.

$$F_I = m_I \frac{d^2X}{dt^2} \tag{4}$$

Here, F_I is the force (N) exerted by the impactor on the airbag, m_I is the mass (kg) of the impactor, and X is the displacement (m) of the impactor in a given time, t (s).

Under ideal conditions for restraint, $|E_A| = |E_I|$, where E_I is the energy released by the impactor and E_A is the energy that should be adsorbed by the airbag. Hence, eqs. (3) and (4) were combined as follows:

$$(P_B - P_A) \cdot A_{eff} = m_I \frac{d^2X}{dt^2} \tag{5}$$

In reality, however, such an ideal condition occurs only when the area of contact between the airbag and the impactor becomes equal to the effective area, A_{eff}, and this lasts only for a very short time.

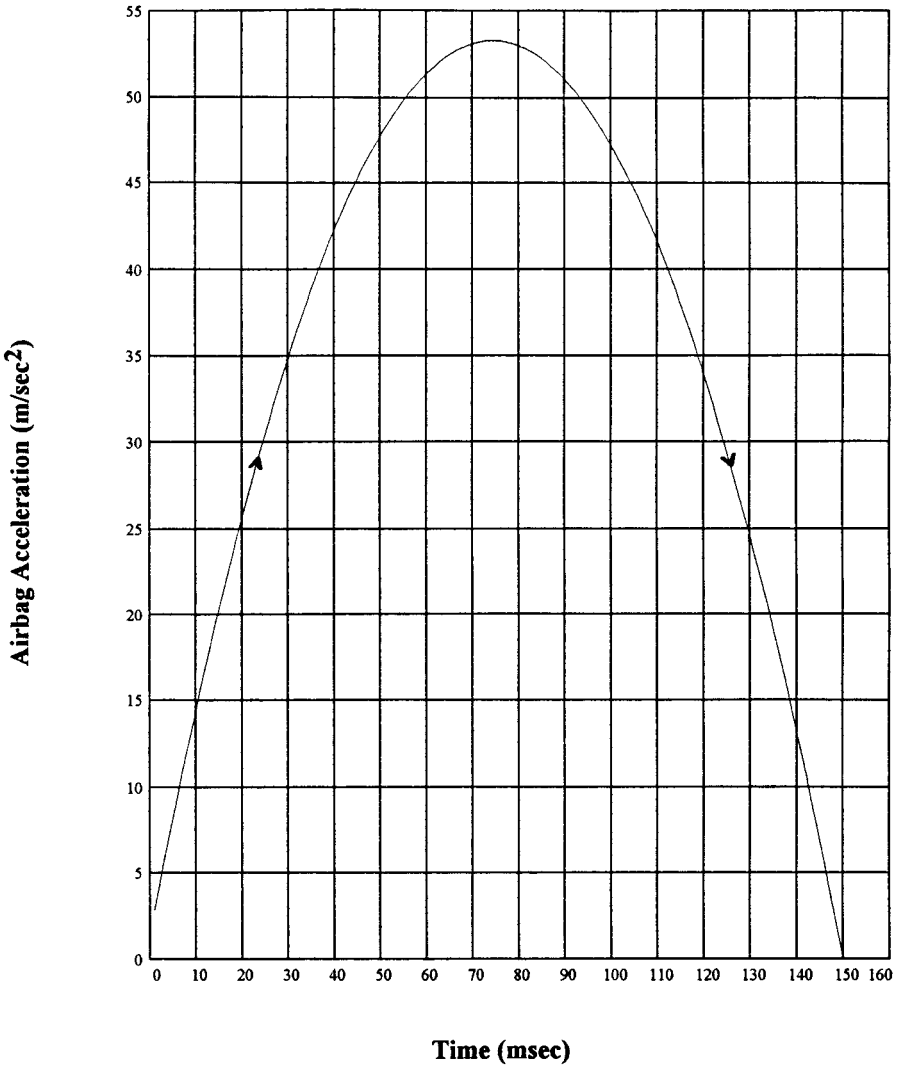

Figure 8 Simulation of airbag acceleration from the airbag module during deployment.

Equation 1 can be written in terms of the displacement change of the impactor and can be solved with eq. (5) to get a differential equation of the following form for change in bag volume:

$$\frac{d^2V_B}{dt^2} = (P_B - P_A)\left(\frac{(A_{eff})^2}{m_I}\right) \tag{6}$$

If P_E is the pressure in the airbag before gas starts to exhaust from the bag, then the bag pressure, P_{B1} (N/m^2), at time, t_1 (s), following an interval, Δt, can be estimated from the total bag pressure loss due to leakage:

$$P_{B1} = P_E - \Delta P_T \tag{7}$$

where ΔP_T is the total bag pressure loss due to leakage (N/m^2) through the entire airbag module.

Under the same condition of no gas exhaust, the relationship between the bag pressure, P_{Bt}, and volume, V_{Bt}, at a certain time, t, and the same relationship between P_E and V_E after a time, $t + \Delta t$, can be estimated from the equation of state. If an ideal gas assumption is used

$$P_{Bt} \cdot V_{Bt} = P_E \cdot V_E \tag{8}$$

Under the exhaust conditions, the gases in an airbag can be released by the viscous flow of gases through the fabric, vents, and seams. An estimate of these three mechanisms can be evaluated

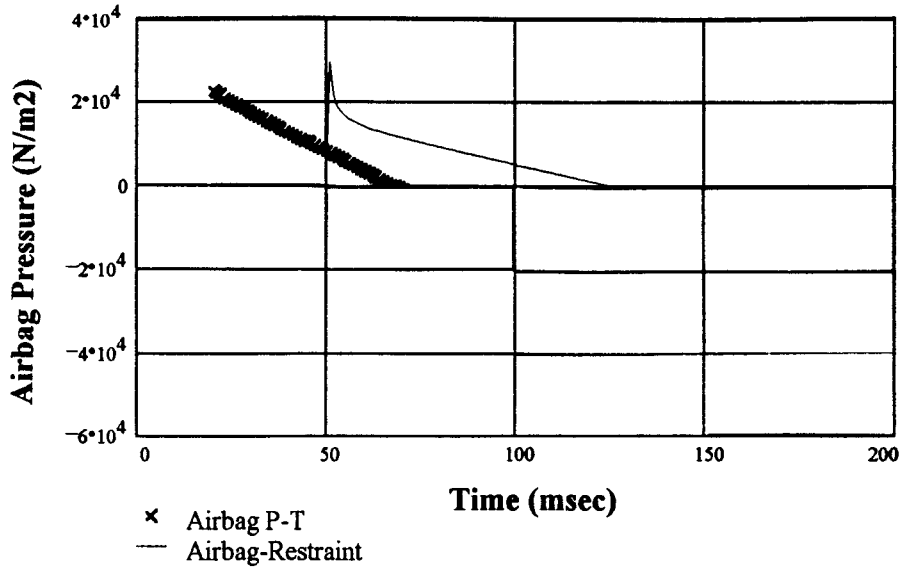

Figure 9 Simulation of the restraint performance of a vented airbag system.

through the kinetic energy adsorption model that uses the parameters estimated from blister inflation.[15,17] Hence, the total leakage in an airbag under the conditions described in this model can be written as follows:

$$\Delta P_T = (\Delta P'_F + \Delta P'_V + \Delta P'_S) \cdot \Delta t \qquad (9)$$

Here, ΔP_T is the combined total pressure loss due to leakage (N/m^2), $\Delta P'_F$ is the pressure loss rate through the permeable fabric ($N\ m^{-2}\ s^{-1}$), $\Delta P'_V$ is the pressure loss rate through the vent ($N\ m^{-2}\ s^{-1}$), and $\Delta P'_S$ is the pressure loss rate through the seam ($N\ m^{-2}\ s^{-1}$) over a time span of Δt (ms). $\Delta P'_V$ and $\Delta P'_S$ can be estimated by the blister-inflation technique; details about this estimation are given in our earlier publication.[15] Solving eqs. (7–9) simultaneously gives an expression for the change in airbag pressure as a function of time

$$\frac{dP_B}{dt} = \left[\frac{P_{Bt}}{V_E}\left(\frac{dV_B}{dt}\right)\right] - (K) \qquad (10)$$

where K is a constant and is equivalent to the quantity $(\Delta P_T/\Delta t)$, because an average value was used from our quasi-steady-state estimation[15] of parameters in eq. (9). The change in bag pressure with time can, therefore, be estimated by solving eq. (10). In our case, a complete numerical simulation was carried out by solving all of the above equations. Outputs from the two models, namely, FMRM and KEAM, were used in the proposed simulation. A systematic integration of these models is shown in Figure 6.

NUMERICAL SIMULATION RESULTS AND DISCUSSIONS

This simple numerical model was used to establish the relationships between various variables that influence restraint on an occupant. The initial conditions used in this model were as follows: the mass of the impactor/occupant is due to the contribution of the passenger's upper body and head; hence, a 30-kg mass was used. A reasonable estimate for the velocity of the passenger toward the airbag was found to be 13 m/s. The total average leakage rate through the vent, seams, and fabric was experimentally determined to be 430 $N\ m^{-2}\ ms^{-1}$ for the vented airbags. In contrast, for the ventless airbag systems, exhaust conditions rely on the fabric, and to a certain extent on seams. In such cases, the average pressure leakage rate was found to be 205 $N\ m^{-2}\ ms^{-1}$. These initial conditions were used throughout this work.

Simulation of Pressure–Time History

Based on the assumption of ideal gas behavior for the inflating gas, the maximum airbag pressure for a given volume of the airbag and the tempera-

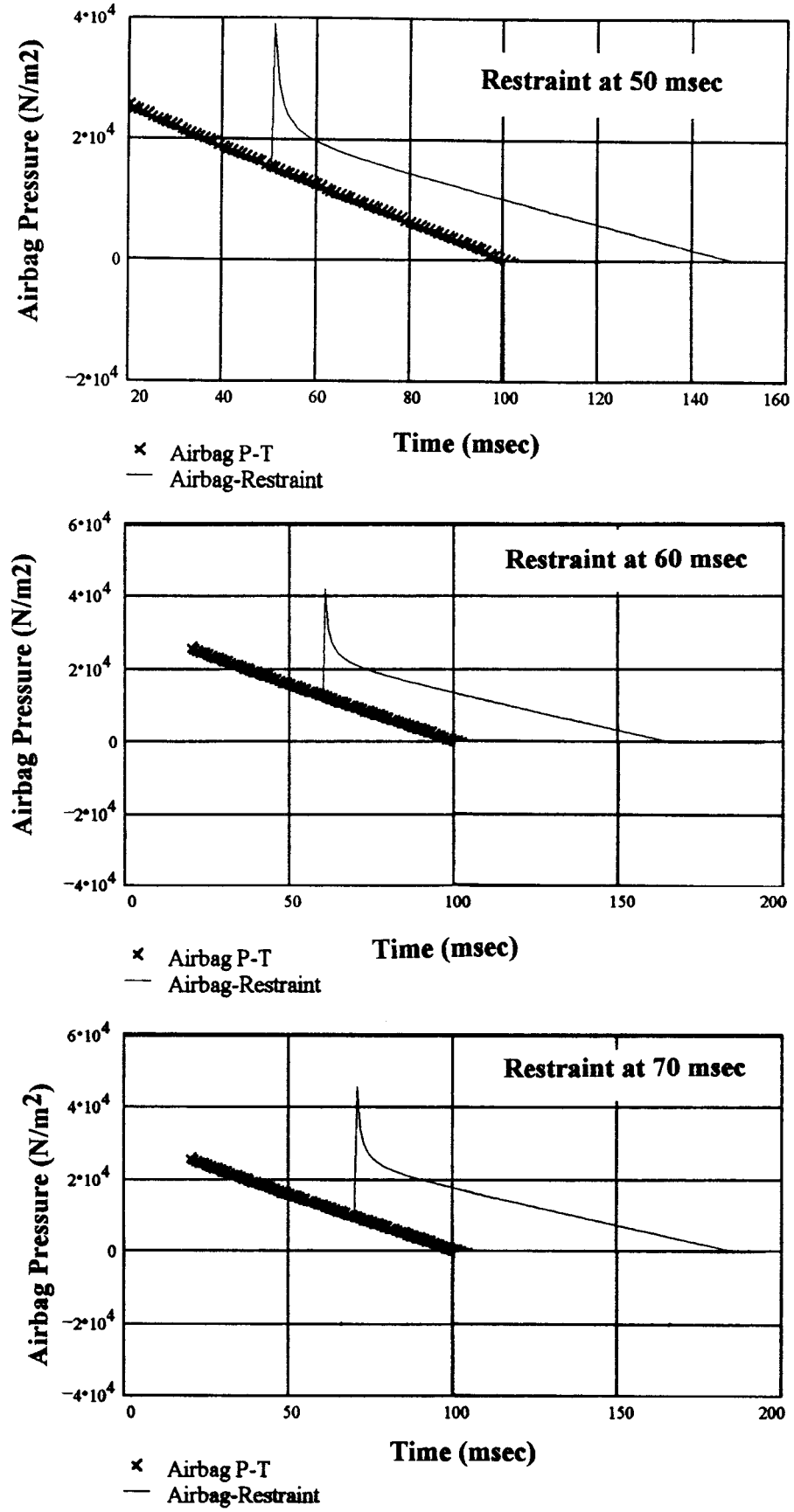

Figure 10 The effect of the time of contact between the airbag and the impactor on the achieved restraint.

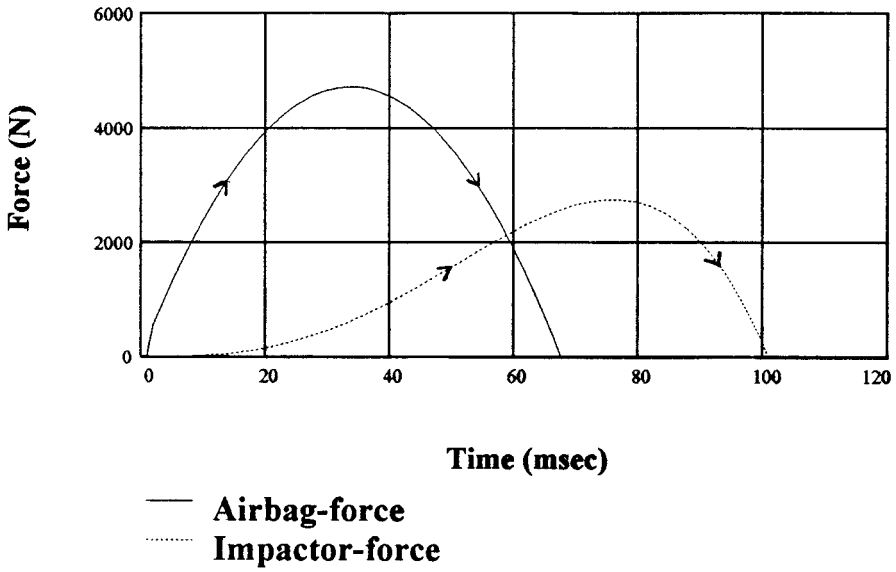

Figure 11 Changes in the interaction forces between the impactor and the airbag with time.

ture of the gas was estimated. The gas leakage characteristics were experimentally determined for each of the fabrics under consideration. Then, from eq. (10), the change in airbag pressure with time was calculated. This approach was used to overcome the high variability observed with the pyrotechnique inflator gas flow equations used in many commercial simulation programs. This pressure–time history without the presence of the impactor is shown in Figure 7. This figure shows only the second peak produced after 30 ms in the pressure–time history. Hence, an initial time of 0 ms corresponds to the 30-ms mark in Figure 1. The effect of the inflating gas temperature on this history is also shown in Figure 7 for gas temperatures of 800 and 400 K. Generally, with an increase in inflating gas temperature, the amount of gas required to inflate the airbag to a certain pressure decreases. From Figure 7, it is clear that inflation gases at 800 K would create a bag pressure of at least 40 kN/m^2 more than if the gas was at 400 K, and it will do so in a much shorter time interval. Also, the elapsed time required for the bag pressure to fall to atmospheric pressure was delayed (more than twice) by increased inflation gas temperature.

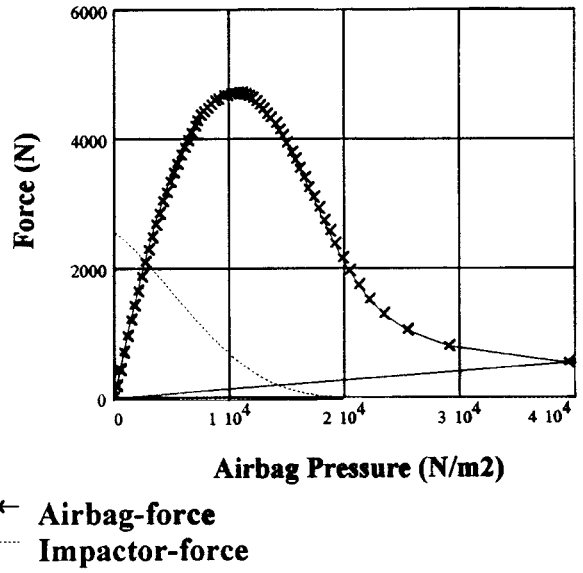

Figure 12 Changes in the interaction forces between the impactor and the airbag with bag pressure.

Airbag–Occupant Restraint

The acceleration of a point on the airbag from its module in the steering column is at a much higher velocity, as shown in Figure 8. The airbag attains an acceleration of 53 m/s^2 during deployment under the simulation conditions. However, from the authors' experience, the velocity of the airbag from the steering column can reach up to 250 mph under extreme conditions. The time of contact between the airbag and the occupant has to be prop-

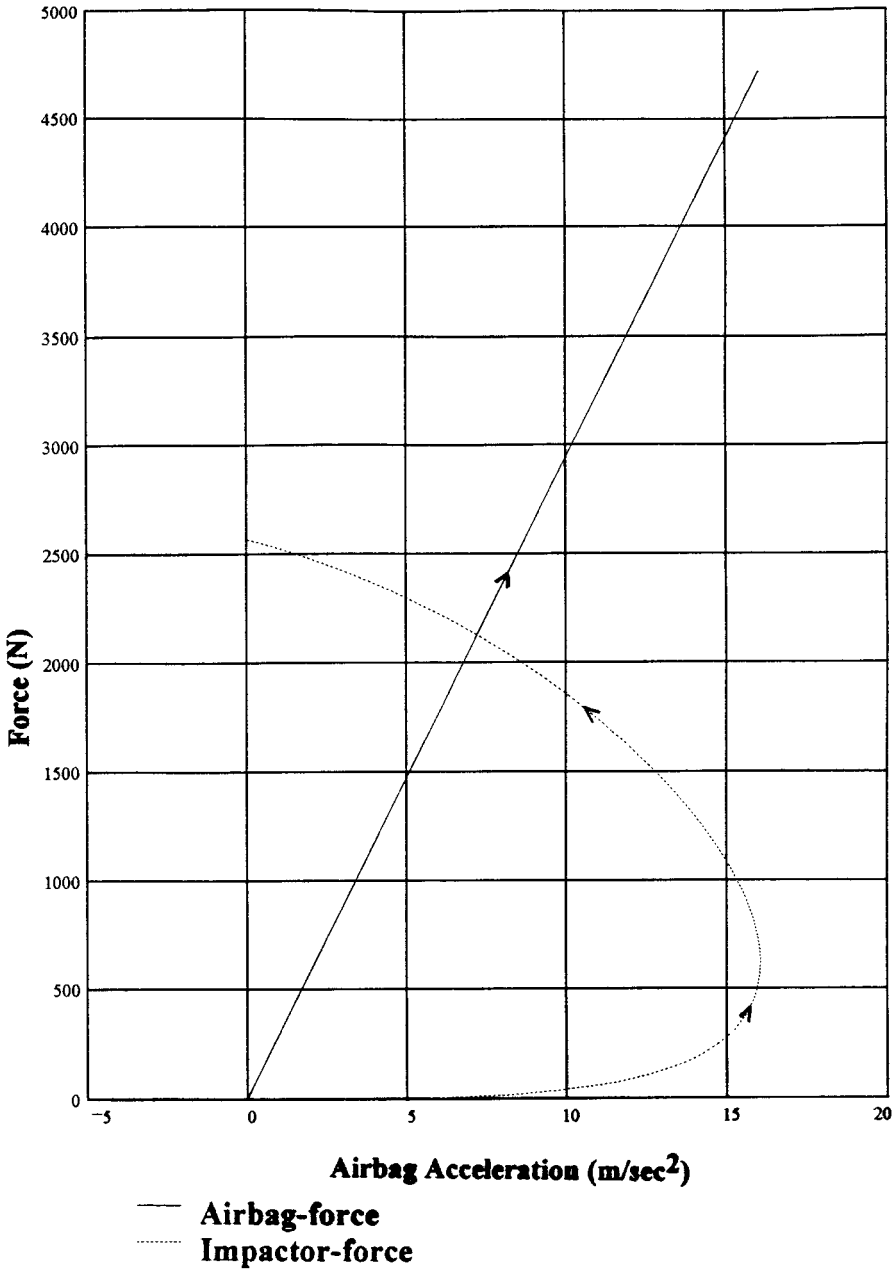

Figure 13 Changes in the airbag-exerted forces with its own acceleration/deceleration during imposed restraint.

erly tuned for the experienced field operating conditions of an airbag.

The simulation was carried out in the presence of the impactor/occupant in order to analyze the restraint action after contact. Figure 9 shows the restraint action of a vented airbag system. The vented airbag pressure reaches atmospheric pressure in about 68 ms when inflated in isolation. A restraint action was imposed after a 50-ms interval, and the response of the model to this restraint is also shown in Figure 9. On contact, the bag pressure increases to about 33 kN/m^2, after which, the time required for the bag pressure to reach atmospheric pressure was extended to 128 ms.

The restraint action imposed at three different time intervals, 50, 60, and 70 ms, along with the original pressure–time history without any im-

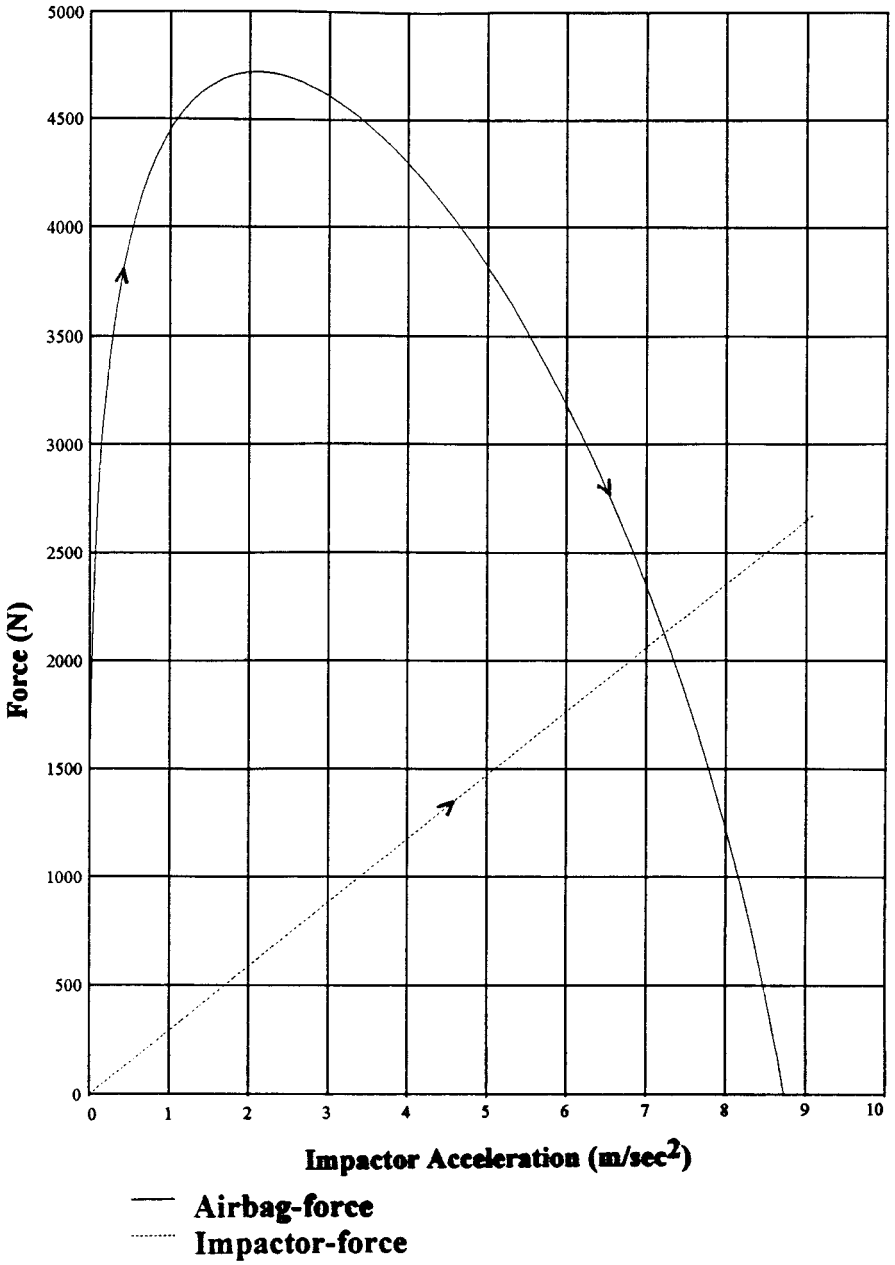

Figure 14 Changes in the impactor-exerted forces with its own acceleration/deceleration during imposed restraint.

pactor for a ventless airbag system, is shown in Figure 10. The bag pressure at the point of contact between the impactor and the airbag was different in each case. It is important to note that with the reduction of airbag pressure at contact, the area below the restraint action curve increased. That is, an increase in the peak pressure and elapsed time was noticed due to the imposed restraint. This should give a better picture of the change in the airbag's exerted force due to a change in time of contact between the airbag and the occupant. This delay, however, apparently does not seem to curtail the achieved restraint.

Analysis of Interaction Forces Between Airbag and the Occupant

The forces of interaction between the impactor and the airbag were analyzed during the restraint

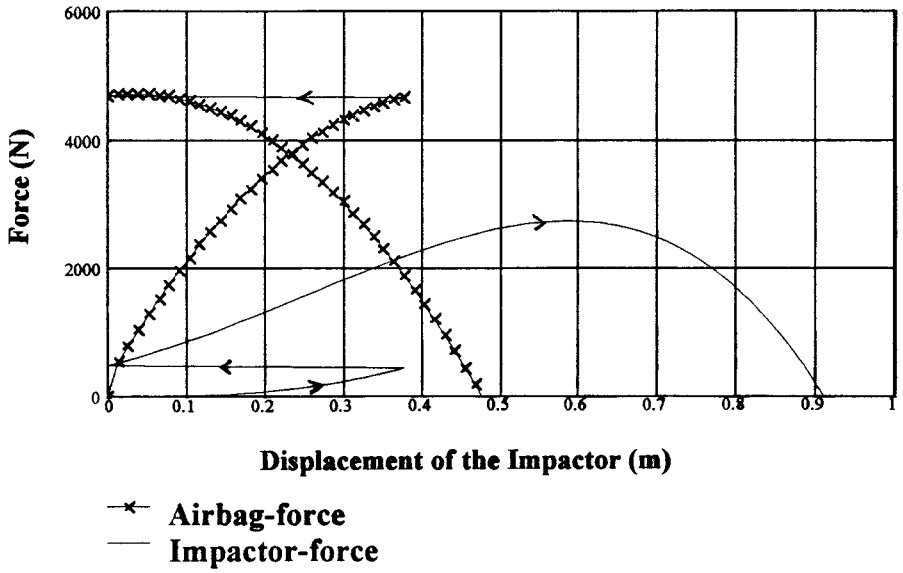

Figure 15 Changes in the interaction forces between the impactor and the airbag with displacement of the impactor.

action of the occupant/impactor. The force exerted by the airbag on the impactor and vice versa were plotted against time, as shown in Figure 11. It should be realized that more than 30–45% of the energy generated by the occupant after impact could be adsorbed by the present steering columns. The simulation results presented here do not take this factor into account. The force exerted by the airbag on the impactor is initially higher than the actual force that the impactor applies on the bag. When the effective area of contact between the passenger and the impactor becomes equal to the area of the impactor itself, however, then an increase in the impactor force is noticed. This phenomenon does not occur immediately

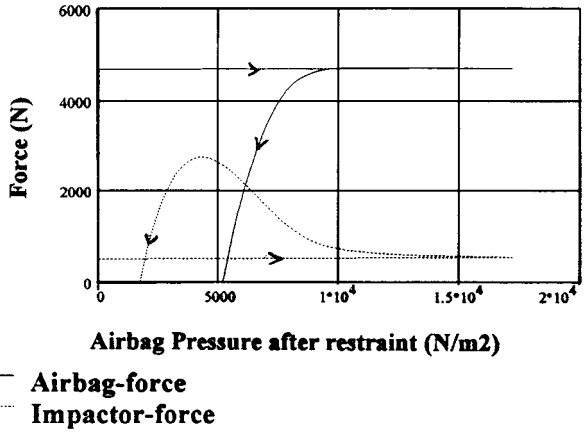

Figure 16 Changes in the interaction forces between the impactor and the airbag with displacement of the impactor after contact between the two.

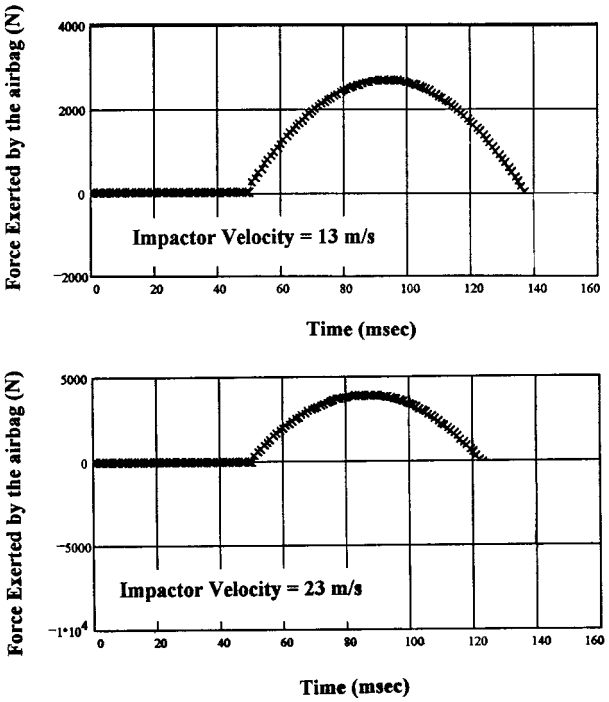

Figure 17 Effect of the impactor velocity on the airbag-generated force.

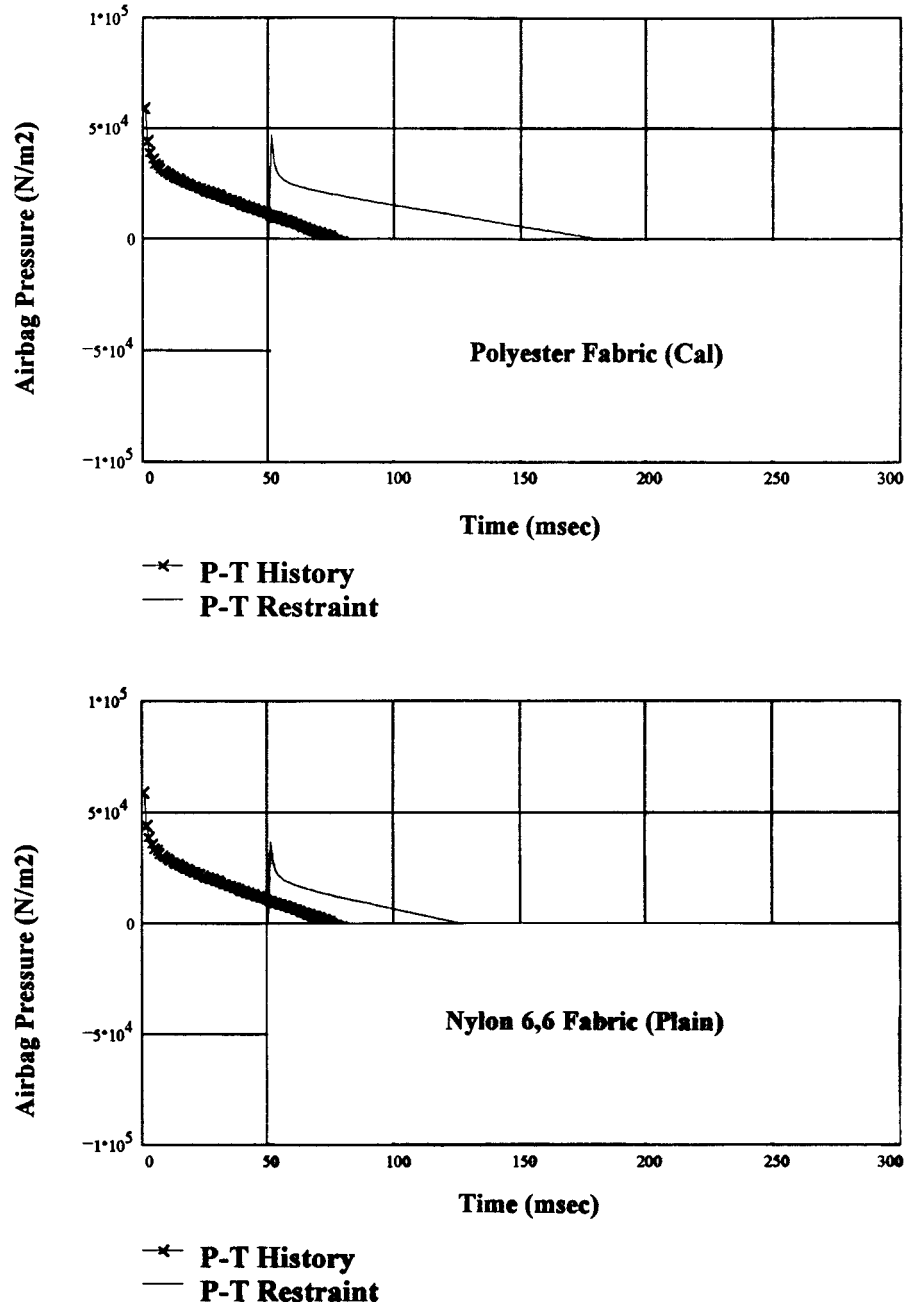

Figure 18 Comparison in performance between airbag woven from a nylon 6,6 fabric (420D-Plain) and a polyester fabric (440D-Calendered).

when both of the areas become identical, but only after a time delay of roughly 8–10 ms. In this period, $|F_A| = |F_I|$, and hence, ideal conditions exist. The maximum force due to the airbag was observed to occur at around 38 ms, after which the bag began to decelerate. On the other hand, the impactor acceleration increases up to a time of 80 ms and reaches zero after 150 ms, as shown in Figure 8. The deceleration of the airbag was found to start at a displacement of 0.37 m. However, it should be realized that the type of reaction surface considered in an analysis would have a substantial effect on the observed forces of interaction.

A plot of the forces of interaction between the airbag and the impactor versus the airbag pres-

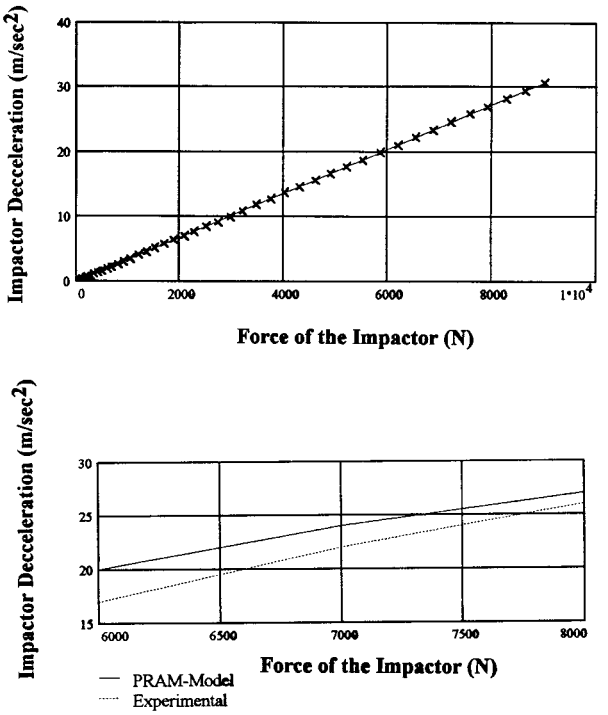

Figure 19 Comparison of PRAM prediction of the impactor force and deceleration changes with experimental data.

sure change is shown in Figure 12. The force exerted by the airbag and the impactor increases at a very slow rate until the effective area of contact between them starts to increase. A restraint action was imposed at a time lapse of 50 ms, and the bag pressure at this point was around 40 kN/m^2. At the onset of contact, the force exerted by the airbag on the impactor increases at a faster rate in comparison to the force exerted by the impactor. When the airbag begins to decelerate, however, the impactor pressure increases before the impactor finally experiences deceleration. A plot of the forces exerted by the airbag and the impactor against their individual accelerations and decelerations is shown in Figures 13 and 14.

A plot of the two types of force changes with displacement of the impactor is shown in Figure 15. The force exerted by the airbag increases until a displacement of 0.37 m by the impactor. After this initial increase, the airbag begins to experience deceleration forces at a much slower rate until the effective area of contact between the two becomes equal to the area of the impactor. Once this stage is reached, the airbag is observed to decelerate at a steady rate. The same phenomenon is observed with the forces exerted by the impactor on the airbag, but at a much lower magnitude, until a total displacement of 0.37 m is reached. After this, the impactor forces increase until the airbag is completely deflated.

The above phenomenon is depicted much more clearly in Figure 16, where the forces encountered during the restraint action alone are graphed against the bag pressure. The individual forces stayed at a constant level until a bag pressure of 17 kN/m^2 was reached in the airbag. The time corresponding to a zero bag pressure occurred at 50 ms, after which the restraint was applied.

The effect of the velocity of the impactor/occupant on the forces generated by the airbag on the impactor was also simulated. The results from this simulation are shown in Figure 17. The simulations shown in this figure are for two different velocities, 13 and 23 m/s. The peak force attained due to the imposed restraint increased from 2800 to 4600 N for the increase in velocity. At a higher impactor velocity (23 m/s), the time required to reach this peak bag force was about 7–10 ms earlier than at 13 m/s im-

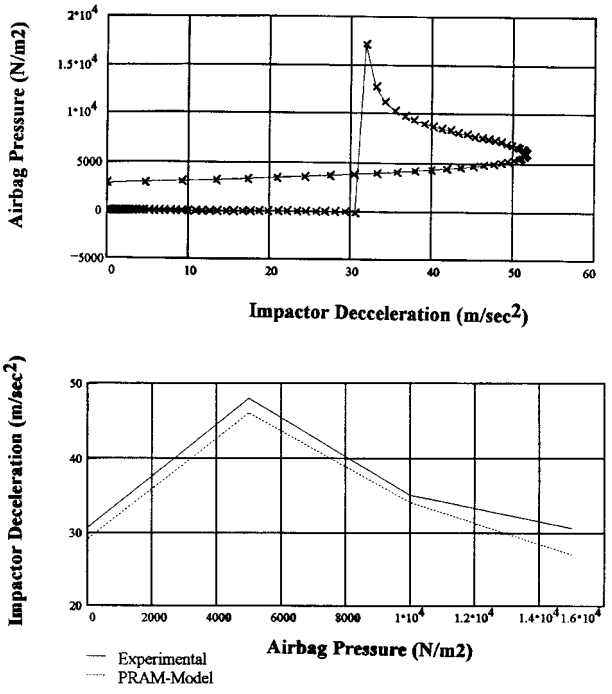

Figure 20 Comparison of PRAM prediction of the bag pressure and impactor deceleration changes with experimental data.

pactor velocity. Also, the bag force decayed to zero in less time (>16 ms) for the higher impactor velocity.

Comparison in Performance of Different Airbags (Nylon 6,6 and Polyester)

The performances of vented airbags constructed from either a 420D nylon 6,6 fabric or a 440D polyester fabric of similar weave count were compared for their restraint behavior. The results from the simulation studies are given in Figure 18 for these two fabrics. With the polyester material, the peak bag pressure due to restraint was higher than that experienced for the bag woven from nylon 6,6 material. Also, the time required for the airbag pressure to reach the atmospheric pressure was greater with the polyester fabric. This is due to their differences in permeability and biaxial extension.[18] However, a close examination of the pressure–time history, without the presence of an impactor, does not show a significant difference. Hence, the importance of the change in the porosity of the fabric, first after the attainment of the initial peak pressure in the airbag and second when the impactor comes in contact with the bag, is apparent. A comparison of the permeability and biaxial deformation of different nylon 6,6, nylon 6, and polyester fabrics of various physical characteristics can be referred to in our earlier publications.[12–18]

Comparison of Numerical Predictions of Passenger Restraint Action Model with Experimental Data

A comparison of the proposed passenger restraint action model (PRAM) predictions with an experimental plot obtained from reference 1 is presented in Figures 19 and 20. A plot of the impactor deceleration with the force exerted by the impactor on the airbag is shown in Figure 19. A comparison of this prediction with the experimental data is presented as a separate plot in the same figure. A reasonably good comparison was obtained considering the level of complexities and assumptions involved.

A similar comparison for the change in the bag pressure once the impactor started to decelerate is shown in Figure 20. In this figure, the impactor comes in contact with the inflating airbag after a 30-ms interval. This was chosen because the published experimental data were available at these conditions. After the onset of contact, the acceleration of the impactor increased further for a very short time span, but with a higher pressure spike. After the attainment of this peak pressure, the impactor began to decelerate. Using this scenario, good comparisons between the model predictions and the published experimental data were observed.

CONCLUSIONS

A variety of numerical simulations of various parameters can be carried out with this proposed simple numerical model, PRAM. For example, an analysis of the forces of interaction between the occupant and the airbag, displacement of the occupant, the acceleration/deceleration of the occupant, and the changes in the bag pressure during the applied restraint were investigated. The influence of all of the above factors on the level of restraint achieved is presented.

This model is very simple to implement and would be helpful for understanding the effect of various airbag-related parameters on energy adsorption. A comparison similar to the driver airbag simulations shown in this article can be easily carried out for a passenger side airbag as well. A good comparison between the proposed PRAM and published experimental data in the literature was observed.

This work was sponsored by the Chrysler Challenge Fund Project No. 2002570 and State of Texas, ATP Project No. 003644-012. It is acknowledged that work of this type could not be completed without the commitment of Chrysler Corporation to vehicle safety.

REFERENCES

1. D. J. Nefske, SAE paper 720426, 1972.
2. J. T. Wang and D. J. Nefske, SAE paper 880654, 1988.
3. R. A. Hammond, SAE paper 710019, 1971.
4. J. T. Johnson, R. E. McComb, T. F. McDonnell, and D. R. Trowbridge, SAE paper 710017, 1971.
5. F. J. Irish, R. A. Potter, and R. D. McKenzie, SAE paper 710015, 1971.
6. B. K. Hamilton, C. Young, C. P. Talley, K. Chakravarthi, D. E. Finlow, and W. H. Wright, SAE paper 720415, 1972.
7. A. I. King, C. C. Chou, and J. A. Mackinder, SAE paper 720036, 1972.
8. J. D. Horsch and C. C. Culver, SAE paper 791029, 1979.

9. R. Keshavaraj, R. W. Tock, and D. Haycock, *J. Textile Inst. (U.K),* **87,** 554 (1996).
10. R. W. Tock and G. S. Nusholtz, SPE, ANTEC' 93, Technical papers, 1302–1306, May 1993.
11. R. W. Tock and G. S. Nusholtz, SPE, ANTEC' 93, Technical papers, **3,** 2480–2486, May 1993.
12. R. Keshavaraj, R. W. Tock, and G. S. Nusholtz, ANTEC' 94, SPE Technical Papers, **3,** 2556–2559, May 1994.
13. R. Keshavaraj, R. W. Tock, and G. S. Nusholtz, *J. Mechanics,* to appear.
14. R. Keshavaraj, R. W. Tock, and G. S. Nusholtz, presented at the Annual Conference of AICHE, San Francisco, Nov. 1994.
15. R. Keshavaraj, R. W. Tock, and G. S. Nusholtz, SAE paper 950340, 1995.
16. R. Keshavaraj, R. W. Tock, and G. S. Nusholtz, *J. Appl. Polym. Sci.,* **57,** 1127 (1995).
17. R. Keshavaraj, R. W. Tock, and G. S. Nusholtz, SAE paper 950341, 1995.
18. R. Keshavaraj, R. W. Tock, and G. S. Nusholtz, *J. Appl. Polym. Sci.,* **61,** 1541 (1996).